

## Competition between proximity-induced superconductivity and pair breaking: Ag sandwiched between Nb and Fe

H. Stalzer,<sup>1</sup> A. Cosceev,<sup>1</sup> C. Sürgers,<sup>1</sup> and H. v. Löhneysen<sup>1,2</sup>

<sup>1</sup>Physikalisches Institut and DFG Center for Functional Nanostructures, Universität Karlsruhe, D-76128 Karlsruhe, Germany

<sup>2</sup>Forschungszentrum Karlsruhe, Institut für Festkörperphysik, D-76021 Karlsruhe, Germany

(Received 12 April 2007; published 13 June 2007)

The magnetization of superconductor and/or normal-metal (Nb/Ag) double layers is investigated in dependence on temperature  $T$  and magnetic field  $B$ . Screening currents in the normal-metal induced by the proximity effect give rise to a diamagnetic transition in a weak magnetic field at a temperature  $T_b$ . The phase transition is suppressed when Fe is in direct contact with Ag. Surprisingly, the diamagnetic signal of Ag is recovered for small Ag film thickness  $d_{\text{Ag}}$ . These findings are qualitatively explained by the competition in the Ag layer between proximity-induced superconductivity by the Nb layer and pair breaking by the ferromagnetic Fe layer.

DOI: 10.1103/PhysRevB.75.224506

PACS number(s): 74.45.+c, 74.25.Ha, 74.78.-w

Heterostructures with superconducting elements, exploiting the macroscopic quantum coherence of the superconductive wave function, have become of increasing interest in recent years. The integration of superconducting materials ( $S$ ) in electronics leads to interface contacts with normal metals ( $N$ ) and also with ferromagnets ( $F$ ) playing an important role in spintronics. The “proximity effect,” i.e., the penetration of the superconductive pair amplitude of  $S$  into the adjacent  $N$  or  $F$  metal, is mediated by the microscopic process of Andreev reflection. At the interface, incident electrons and retroreflected holes form correlated but mutually independent Andreev pairs over a coherence length  $\xi_N(T)$ . The relevant length scales for a  $S/N$  system, where  $S$  is considered as infinitely thick, are the electron mean free path  $l_N$ , the thickness  $d_N$ , and  $\xi_N(T)$ .

Early investigations of the proximity effect in thin  $S/N$  double layers have focused on measurements of their transition temperatures. These experiments could be well described by the quasiclassical approach<sup>1</sup> in the “dirty limit,” i.e., for  $l_N \ll (d_N, \xi_N)$ . The magnetic properties, e.g., the diamagnetic response, of  $S/N$  systems in an external magnetic field  $B$  have been investigated theoretically and experimentally.<sup>2–7</sup> For commercial sheets and wires, the data clearly deviate from the dirty-limit behavior.<sup>4,7,8</sup> In particular, data obtained on well-annealed coaxial Nb/Ag wires<sup>9</sup> are better described by taking into account the large  $l_N$ , i.e., considering the “ballistic regime.” Besides, a paramagnetic re-entrance behavior was observed at low temperatures.<sup>10,11</sup> The dirty or clean limits are characterized by different temperature dependences of  $\xi_N$ , i.e.,  $\xi_N^d(T) = (\hbar v_F l_N / 6\pi k_B T)^{1/2}$  and  $\xi_N^c(T) = \hbar v_F / 2\pi k_B T$ , respectively.<sup>3</sup> Measurements of the magnetization  $M(T, B)$  allow the determination of the critical field  $B_b(T)$  and the characteristic Andreev temperature  $T_A = \hbar v_F / 2\pi k_B d_N$  of the  $N$  layer, defined by  $\xi_N(T_A) = d_N$ .  $B_b$  and  $T_A$  can be considered as parameters reflecting the stability of the proximity-induced superconductivity (PIS) in  $N$ .

While previous experiments focused on commercial  $S/N$  sheets and wires, little is known about the magnetic response of clean  $S/N$  double layers with thickness  $d_N$  in the sub-micrometer range in contact with a ferromagnetic layer. In  $S/F$  contacts, the pair amplitude in  $F$  decays exponentially with distance from the interface, superposed with a periodic

modulation due to the ferromagnetic exchange interaction  $I_{\text{ex}}$ .<sup>12–14</sup> In particular, for strong ferromagnets with  $I_{\text{ex}}\tau > \hbar$  ( $\tau$ , elastic-scattering time), the pair-condensate amplitude decays on a length scale of the order of the electron mean free path  $l_F$  in  $F$ .<sup>15</sup> Cladding of micrometer-thick coaxial Nb/Cu wires with Fe results in a strong depression of the proximity effect.<sup>5</sup> In  $S/N$  systems the diamagnetic transition of the  $N$  layer shifts to higher temperatures with decreasing  $d_N$  indicating an enhanced stability of PIS, whereas the cladding of the outer  $N$  surface by a ferromagnetic metal gives rise to additional pair breaking. Hence, in  $S/N/F$  systems with appropriate  $N$  layer thickness, a concurrent influence of PIS and pair breaking by  $F$  on  $N$  should be observed, as will be demonstrated in this paper. We report on magnetization measurement on high-quality Nb/Ag double layers with  $d_{\text{Ag}} < 1 \mu\text{m}$  and with a finite but long  $l_{\text{Ag}}$  of the order of  $d_{\text{Ag}}$ . We observe a diamagnetic phase transition of the Ag layer at a temperature  $T_b$  depending on  $B$  and  $d_{\text{Ag}}$  from which we determine  $B_b$  and  $T_A$ . In particular, we focus on Nb/Ag/Fe triple layers and find that for thick Ag layers, the diamagnetic screening in Ag is suppressed by the proximity of Fe. On the other hand, for small  $d_{\text{Ag}}$ , the diamagnetic signal in Ag reappears due to a delicate balance between PIS in Ag and pair breaking in contact with the ferromagnetic Fe.

The samples were epitaxially grown by electron-beam evaporation in ultrahigh vacuum (base pressure  $1 \times 10^{-10}$  mbar). Nb was deposited with a fixed thickness of 200 nm on (11 $\bar{2}$ 0)-oriented sapphire substrates (width  $w = 0.7\text{--}5$  mm, length  $L = 4\text{--}8$  mm) at a substrate temperature  $T_S = 920$  K and covered by 35–550 nm Ag at  $T_S = 470$  K. The crystalline quality was checked by *in situ* reflection high-energy electron diffraction (RHEED) and *ex situ* by x-ray diffraction, indicating growth directions of Ag[111]||Nb[110] with mosaic spreads of 0.65° and 0.78° for Nb and Ag, respectively. 40 nm Fe were deposited onto the Ag layer at room temperature without further annealing. For some films, a SiO<sub>2</sub> barrier was introduced between the Ag and Fe layers. The observed RHEED streaks indicate a smooth growth of Fe along [110] on Ag(111). The in-plane magnetization of the Fe layer was checked by vibrating-sample magnetometry yielding a Fe moment of  $m_{\text{Fe}} = (2.1 \pm 0.1)\mu_B$  in agreement with that of bulk Fe, see Fig. 1 (inset). A coercivity of

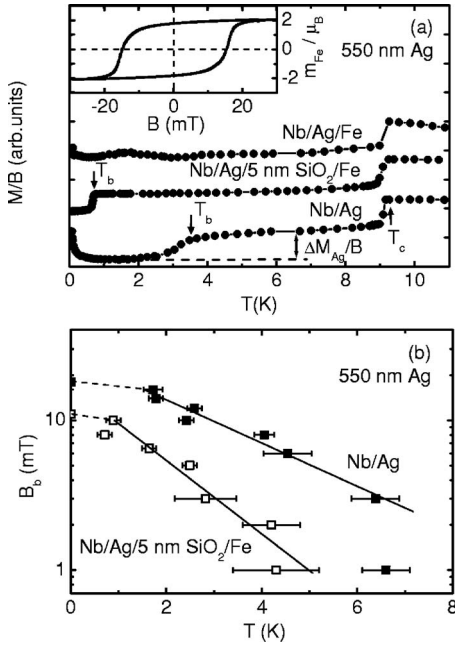


FIG. 1. (a)  $M(T)/B$  for samples with  $d_{\text{Ag}}=550$  nm and  $d_{\text{Fc}}=40$  nm in a field of  $B=8$  mT.  $T_c$  and  $T_b$  indicate the diamagnetic transition of the Nb and Ag layers, respectively. Inset shows the magnetization curve of the Nb/Ag/Fe sample taken at  $T=10$  K. (b) Semilogarithmic plot of  $B_b(T)$ . Solid lines indicate a behavior  $\ln B_b \propto -T/T_A$ . Dashed lines serve as guides to the eye toward  $B_b(0)$ .

$\approx 15$  mT was obtained for all Nb/Ag/Fe triple layers. The samples were, finally, covered by 5 nm  $\text{SiO}_2$  or Si to protect them from oxidation in ambient air.

Four-point measurements of the residual resistivity  $\rho_{\text{Nb}}$  and of the upper critical field on a single 200 nm Nb film yield an electron mean free path  $l_{\text{Nb}}=27$  nm using<sup>16</sup>  $\rho_{\text{Nb}}l_{\text{Nb}}=3.75 \times 10^{-16}$   $\Omega$  cm<sup>2</sup> and an upper critical field  $B_{c2}(2\text{ K})=0.65$  T. The following superconducting parameters were obtained from standard BCS relations and material parameters of bulk Nb:<sup>16,17</sup> coherence length  $\xi_{\text{Nb}}=19$  nm; penetration depth  $\lambda_{\text{Nb}} \approx 42$  nm  $< d_{\text{Nb}}$ ; lower critical field  $B_{c1}(2\text{ K})=64$  mT. Since  $d_{\text{Nb}} \gg (\lambda_{\text{Nb}}, \xi_{\text{Nb}})$ , the  $S$  layer can be regarded as infinitely thick. From resistance measurements on several Nb/Ag double layers with the current in plane, a lower limit  $l_{\text{Ag}}^{\text{min}} \approx d_{\text{Ag}}$  was estimated in comparison with the single Nb film. The magnetization  $M$  at constant  $B$  was measured as a function of  $T$  in a coaxial  $dB_z/dz$  gradiometer coupled to a superconducting quantum interference device (SQUID). After cooling down in zero magnetic field to temperatures of about 60 mK, magnetization signals  $M(T)$  were recorded during warm-up. A homogeneous and stable magnetic field was applied nearly parallel to the sample surface by magnetic-flux enclosure of an external magnetic field, using a superconducting Pb or NbTi/Nb/Cu cylinder<sup>18</sup> surrounding the sample holder. Although care was taken to measure all samples at similar positions in the gradiometer, an absolute measurement of the magnetization was not possible due to the strong dependence of the Nb signal from a possible tilt angle between film plane and field, which could be controlled only to  $\pm 0.5^\circ$ .<sup>19</sup> Therefore, the  $M/B$  data are given in

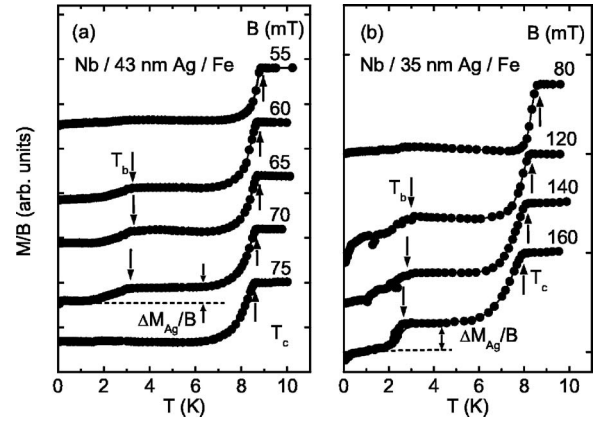


FIG. 2.  $M(T)/B$  of Nb/Ag/Fe samples with  $d_{\text{Fc}}=40$  nm for different  $d_{\text{Ag}}$  and applied fields  $B$ . See text for details.

arbitrary units. After each  $M(T)$  cycle at constant field, the superconducting cylinder was heated to well above its transition temperature for complete expulsion of trapped magnetic flux.

Figure 1(a) shows  $M(T)/B$  of a Nb/Ag double layer with  $d_{\text{Ag}}=550$  nm. The sharp diamagnetic signal at  $T_c \approx 9.1$  K is due to the superconducting transition of the Nb layer. At a lower temperature  $T_b$ , a further diamagnetic transition of height  $\Delta M_{\text{Ag}}/B$  occurs which is attributed to the proximity-induced diamagnetic screening currents in the Ag layer. [The paramagnetic signal at  $T < 300$  mK is due to the oxidized surface of the copper sample holder. This signal is absent in subsequent measurements made with a silver sample holder, see, e.g., Fig. 1(a) (middle curve) or Fig. 2]. We mention that with increasing magnetic field, the transition at  $T_b$  becomes sharper and shifts toward lower temperatures. This sharpening is observed for all samples studied. For the present samples with small  $d_{\text{Ag}}$ , the transition occurs at a few Kelvin and is, therefore, broadened by the temperature-dependent penetration depth  $\lambda_{\text{Ag}}(T)$ .<sup>20</sup> The sharpening of the transition in increasing fields is also inferred from the calculated nonlinear susceptibility of  $S/N$  double layers.<sup>3</sup>

The discrete energy levels of Andreev bound states in  $N$  are given by<sup>2</sup>

$$E_n = \frac{\hbar v_x}{4d_N} \left[ (2n+1)\pi - \frac{2\pi}{\phi_0} \oint \vec{A}(\vec{r}) d\vec{r} \right] \quad (1)$$

( $v_x$ , component of Fermi velocity perpendicular to the interface;  $\vec{A}$ , vector potential;  $\phi_0$ , superconducting flux quantum). For  $T \ll T_A$  and  $B \ll B_b$ , each Andreev pair contributes coherently to the macroscopic screening current because only the lowest Andreev level is occupied. At temperatures above  $T_A$ , the coherence is continuously destroyed by inelastic-scattering events and thermal excitations, changing the population of the Andreev states. In addition, in a magnetic field, the Andreev pairs acquire an additional phase shift by the vector potential according to Eq. (1) leading to a randomization of the Andreev currents and the destruction of the coherence at the critical field  $B_b(T)$ .

The  $B_b(T)$  phase diagram in Fig. 1(b) is in qualitative

agreement with thermodynamic calculations for the clean limit, as previously reported for coaxial Nb/Ag wires.<sup>20,21</sup> The  $B_b(T)$  dependence for temperatures  $T \geq T_A$ , i.e., when  $\xi_{Ag} < d_{Ag}$ , nicely obeys a behavior  $\ln B_b \propto -T/T_A$ , in contrast to the dirty limit where  $\ln B_b \propto -\sqrt{T}$ . For  $d_{Ag}=550$  nm, the  $B_b(T)$  behavior can be described only partly by the dirty limit by using a very long  $l_{Ag}=105$  nm violating the condition  $l_{Ag} \ll \xi_{Ag}$ . The characteristic temperature  $T_A$  obtained from the slope of  $B_b(T)$  (Ref. 20) is  $T_A=3.02$  K, in very good agreement with the theoretical value of 3.06 K estimated from  $T_A=1680$  K nm/ $d_{Ag}$ . While our data show semiquantitative agreement with the thermodynamic phase diagram, we should point out that we actually measure the superheated field  $B_{sh}(T)$ , which may be somewhat larger than the thermodynamic critical field for PIS in Ag. In summary, the Nb/Ag data are quite well described by theory for the clean limit, although the smooth transitions are not expected for first-order transitions. Hence, the films should be classified to fall in the ballistic regime.

In what follows, we focus on the pair-breaking effect by a ferromagnetic Fe layer on the PIS. Deposition of a 40 nm thick Fe layer directly onto Ag with  $d_{Ag}=550$  nm suppresses the diamagnetic signal down to below the lowest temperature of  $\approx 60$  mK, see Fig. 1(a), even in a weak external field of 0.5 mT (not shown). The small signal variations are caused by thermal instabilities of the SQUID system during that measurement. As already mentioned, in  $S/F$  contacts, the pair amplitude in  $F$  decays exponentially with distance from the interface. This is also expected for the Andreev pairs penetrating into the ferromagnetic layer from the “normal conducting”  $N$  layer in a  $S/N/F$  structure. The Andreev pairs experience an additional phase shift in Fe, which destroys the phase coherence in Ag. This has also been reported earlier for coaxial (165  $\mu\text{m}$  Nb/27  $\mu\text{m}$  Cu/0.09  $\mu\text{m}$  Fe) wires.<sup>5</sup> An alternative explanation might be the presence of a magnetic stray field from domain walls, which is minimized only for fields above the coercive field.

For another sample, a 5 nm thick insulating  $\text{SiO}_2$  layer was first deposited on top of the Ag layer before deposition of 40 nm Fe. As expected, the influence of the Fe layer is considerably weakened and a diamagnetic signal of Ag reappears. However, as Fig. 1(a) shows, the diamagnetic transition of Ag appears at a much lower  $T_b$  when compared to the Nb/Ag double layer. The destructive effect of Fe on the proximity effect in Ag also gives rise to a lower  $T_A=1.86$  K and  $B_b(0)=11$  mT [Fig. 1(b)] compared to  $T_A=3.02$  K and  $B_b(0)=18$  mT obtained for the Nb/Ag double layer. The Andreev pairs have a finite probability to tunnel into Fe via  $\text{SiO}_2$  and back again, so that their phase coherence is compromised by  $I_{ex}$  of Fe. In addition, pinholes in the oxide barrier may play a role. Both effects lead to a reduced stability of PIS against magnetic and thermal perturbations. In other words, for a fixed temperature, smaller external fields are sufficient for the destruction of coherence<sup>22</sup> in comparison with Nb/Ag double layers.

Surprisingly, diamagnetic screening by Ag *without* a  $\text{SiO}_2$  barrier reappears in Nb/Ag/Fe samples with much smaller  $d_{Ag}=35$  and 43 nm in a certain range of magnetic field. Figure 2 clearly shows transitions around 3 K, which shift only

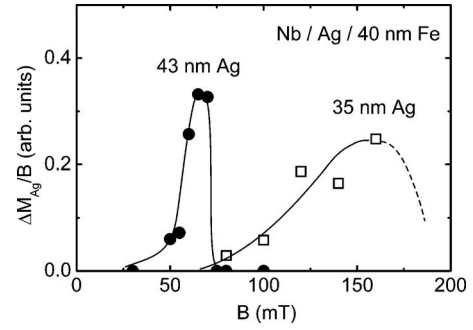


FIG. 3.  $\Delta M_{Ag}/B$  vs  $B$  of Nb/Ag/Fe samples with  $d_{Fe}=40$  nm and different  $d_{Ag}$ . Lines are guides to the eye.

slightly to lower temperatures with increasing field  $B$  together with an increase of the jump  $\Delta M_{Ag}/B$ . Moreover, the fields where the transitions are observed are much larger than the upper limit for the Nb/Ag samples discussed above. At these large values,  $T_c$  of the Nb layer is already reduced. Furthermore, a broadening of the transition is observed due to the flux penetration for fields exceeding the lower critical field  $B_{c1}$ . Figure 3 displays the height of the diamagnetic jump  $\Delta M_{Ag}/B$  vs magnetic field  $B$  for the different samples in order to illustrate the reappearance of the diamagnetic signal of Ag for certain magnetic fields.

One could argue that the effect is due to the presence of a magnetic stray field from the Fe layer. Although a thin magnetic layer does not exhibit a stray field close to the surface plane, a stray field arising from surface roughness<sup>23</sup> or generated by the domain structure of the ferromagnetic layer<sup>24</sup> can play a role. At this point, we cannot conclusively dismiss the possibility that the reappearance of the PIS in a higher applied magnetic field is due to the disappearance of the domains leading to suppression of the stray field. We also cannot exclude effects due to the flux trapped by the Nb layer cooled in the presence of such stray fields. However, the effect of a magnetic stray field from the Fe layer on the diamagnetic screening in Ag is considered to be negligible, as confirmed by zero-field measurements with a magnetized Fe layer; i.e., after complete demagnetization of the field coil, no diamagnetic signal of Nb or Ag was observed. We also mention that the Ag layer shows a complete Meissner effect (not shown) and, therefore, cannot contribute to any flux pinning.

The observed diamagnetic screening of Nb/Ag/Fe triple layers with thin  $d_{Ag}$  cannot be explained by present theories for semi-infinite  $S/N$  bilayers, since some initial assumptions are not valid. For instance, the variation of the superconducting energy gap  $\Delta$  of  $S$  across the  $S/N$  interface cannot be approximated anymore by a step function because  $d_{Ag} \approx \xi_{Nb}$ . Moreover, the effect of pair breaking due to the contact with a F layer is not considered. However, the result can be at least qualitatively explained in the following way. For  $d_{Ag}=35$  and 43 nm, the Andreev energy corresponds to  $T_A=48$  and 39 K, respectively, so that the coherence in the Ag layer will not be destroyed in contact with the ferromagnetic Fe layer. Theoretically, the lowest-energy state ( $n=0$ ) at perpendicular incidence (maximum  $v_x$ ) with respect to the interface would lie above the Fermi energies  $E_F$  of 21 and

17 meV, respectively [Eq. (1)], and well above  $\Delta=1.2$  meV of Nb. No bound Andreev levels exist for trajectories with small incident angles with respect to the interface normal. The finite spin polarization in Fe and the external field  $B$  cause a shift of the Andreev levels to lower energies. The occupation of these levels gives rise to diamagnetic screening currents by correlated phase-coherent Andreev pairs. The magnitude of the diamagnetic signal is also determined by the density of Andreev pairs. Higher densities can be reached by increasing the total number of states between  $E_F$  and  $E_F+\Delta$  with increasing  $B$ . The height of the jump  $\Delta M_{\text{Ag}}/B$  also increases with increasing magnetic field until it vanishes above fields, which completely destroy the phase coherence. Roughly speaking, the PIS in Ag is stabilized for thinner  $d_{\text{Ag}}$  (higher  $T_A$ ) but at the same time, it is weakened by the pair breaking due to the contact with Fe. The balance between these effects can lead to the observation of a diamagnetic transition in Ag for certain  $d_{\text{Ag}}$  and  $B$ . This behavior is visualized in Fig. 3. The external magnetic field  $B$  acts on both Nb and Ag layers, whereas the pair breaking of Fe only acts on the Ag layer. In this picture, it is clear that for a constant thickness  $d_{\text{Ag}}$ , the transition temperature  $T_b$  becomes almost independent of  $B$  due to the strong internal magnetic field in Fe which is some orders of magnitude larger than the external field  $B$ .

In strong ferromagnets with  $l_{\text{ex}}\tau > h$ , such as Fe, the condensation amplitude decays on length scales of the order of  $l_{\text{Fe}}$ .<sup>15</sup> This suggests that for  $l_{\text{Fe}} \geq d_{\text{Fe}}$ , the coherence can be

maintained over the whole layer thickness. Indeed, comparison of the resistivities of different Nb/Ag/Fe films yields lower limit for the mean free path  $l_{\text{Fe}}^{\text{min}} \approx d_{\text{Fe}}$ . Therefore, the coherence of the Andreev pairs is not destroyed despite the large thickness  $d_{\text{Fe}}$ . Pair breaking by spin-flip scattering can be neglected, since at low temperatures single Fe spins can hardly be flipped against the exchange field of their surrounding.<sup>25</sup>

In conclusion, we have observed a diamagnetic screening of the normal metal in high-quality Nb/Ag double layers with large electron mean free paths  $l_{\text{Ag}}$ . For thick Ag layers with  $d_{\text{Ag}} \gg (\xi_{\text{Nb}}, \lambda_{\text{Nb}})$ , an additional Fe layer on top of Ag destroys the coherence of Andreev pairs. However, the diamagnetic signal of Ag is recovered if the Ag layer thickness is strongly reduced. This is due to the competition of induced superconductivity by Nb and pair breaking by Fe. This qualitative interpretation requires further theoretical investigations. Finally, we wish to point out that the proximity effect in  $S/N/F/S$  contacts may be used in order to realize a tunable  $\pi$  contact by application of an external magnetic field.

The authors gratefully acknowledge valuable discussions with W. Belzig, M. Eschrig, P. Wölfle, and A. C. Mota. This work was partly supported by the Graduiertenkolleg ‘‘Angewandte Supraleitung.’’ They thank the Nippon Steel Corporation for providing the NbTi/Nb/Cu cylinder used in the SQUID system.

- 
- <sup>1</sup>For a review of early work, see G. Deutscher and P. de Gennes, in *Superconductivity*, edited by R. D. Parks (Dekker, New York, 1969).
- <sup>2</sup>A. D. Zaikin, *Solid State Commun.* **41**, 533 (1982).
- <sup>3</sup>W. Belzig, C. Bruder, and G. Schön, *Phys. Rev. B* **53**, 5727 (1996).
- <sup>4</sup>A. C. Mota, P. Visani, and A. Pollini, *J. Low Temp. Phys.* **76**, 465 (1989) and references therein.
- <sup>5</sup>Th. Bergmann, K. H. Kuhl, B. Schröder, M. Jutzler, and F. Pobell, *J. Low Temp. Phys.* **66**, 209 (1987).
- <sup>6</sup>Yu. N. Ovchinnikov, B. I. Ivlev, R. J. Soulen, J. H. Claasen, W. E. Fogle, and J. H. Colwell, *Phys. Rev. B* **56**, 9038 (1997).
- <sup>7</sup>Y. Oda and H. Nagano, *Solid State Commun.* **35**, 631 (1980).
- <sup>8</sup>A. Sumiyama, T. Endo, Y. Nakagawa, and Y. Oda, *J. Phys. Soc. Jpn.* **70**, 228 (2001).
- <sup>9</sup>F. B. Müller-Allinger, A. C. Mota, and W. Belzig, *Phys. Rev. B* **59**, 8887 (1999).
- <sup>10</sup>P. Visani, A. C. Mota, and A. Pollini, *Phys. Rev. Lett.* **65**, 1514 (1990).
- <sup>11</sup>F. B. Müller-Allinger and A. C. Mota, *Phys. Rev. Lett.* **84**, 3161 (2000).
- <sup>12</sup>A. I. Buzdin and M. V. Kupriyanov, *JETP Lett.* **52**, 487 (1990).
- <sup>13</sup>Z. Radović, M. Ledvij, L. Dobrosavljević-Grujić, A. I. Buzdin, and J. R. Clem, *Phys. Rev. B* **44**, 759 (1991).
- <sup>14</sup>T. Kontos, M. Aprili, J. Lesueur, and X. Grison, *Phys. Rev. Lett.* **86**, 304 (2001).
- <sup>15</sup>F. S. Bergeret, A. F. Volkov, and K. B. Efetov, *Phys. Rev. B* **65**, 134505 (2002).
- <sup>16</sup>H. W. Weber, E. Seidl, C. Laa, E. Schachinger, M. Prohammer, A. Junod, and D. Eckert, *Phys. Rev. B* **44**, 7585 (1991).
- <sup>17</sup>M. Tinkham, *Introduction to Superconductivity* (McGraw-Hill, New York, 1996).
- <sup>18</sup>I. Itoh and T. Sasaki, *IEEE Trans. Appl. Supercond.* **3**, 177 (1993).
- <sup>19</sup>H. Stalzer, A. Cosceev, C. Sürgers, H. v. Löhneysen, J.-M. Brosi, G.-A. Chakam, and W. Freude, *Appl. Phys. Lett.* **84**, 1522 (2004).
- <sup>20</sup>A. L. Fauchère and G. Blatter, *Phys. Rev. B* **56**, 14102 (1997).
- <sup>21</sup> $B_b(0)$  was determined by the lowest field for which no diamagnetic screening signal was observed down to the lowest temperature of 60 mK.
- <sup>22</sup>M. Zareyan, W. Belzig, and Yu. V. Nazarov, *Phys. Rev. Lett.* **86**, 308 (2001).
- <sup>23</sup>S. Demokritov, E. Tsymbal, P. Grünberg, W. Zinn, and I. K. Schuller, *Phys. Rev. B* **49**, 720 (1994).
- <sup>24</sup>A. Yu. Aladyshkin, A. I. Buzdin, A. A. Fraerman, A. S. Mel'nikov, D. A. Ryzhov, and A. V. Sokolov, *Phys. Rev. B* **68**, 184508 (2003).
- <sup>25</sup>C. Strunk, C. Sürgers, U. Paschen, and H. v. Löhneysen, *Phys. Rev. B* **49**, 4053 (1994).